CTH-RF-196

THESIS FOR THE DEGREE OF DOCTOR OF PHILOSOPHY

Pulsed Neutron Activation for Determination of Water Flow in Pipes

HÅKAN MATTSSON

Nuclear Engineering
CHALMERS UNIVERSITY OF TECHNOLOGY
Göteborg, Sweden, 2005

Pulsed Neutron Activation for Determination of Water Flow in Pipes
HÅKAN MATTSSON
ISBN 91-7291-719-9

Doktorsavhandling vid Chalmers tekniska högskola
Ny serie nr 2401
ISSN 0346-718x

Nuclear Engineering
Chalmers University of Technology
SE-412 96 Göteborg
Sweden
Telephone +46(0)31 772 10 00
Web: www.nephy.chalmers.se

Chalmers Reproservice
Göteborg, Sweden 2005

Pulsed Neutron Activation for Determination of Water flow in Pipes

HÅKAN MATTSSON
Nuclear Engineering
Chalmers University of Technology

ABSTRACT

In a Pulsed Neutron Activation (PNA) flowmeter neutron induced activity is used to measure water flow in pipes. The water in the pipe is bombarded with neutron pulses which introduce activity into the pipe. The activity is then transported and mixed with the flow. Gamma radiation emitted from the activity is measured with a detector downstream from the activations point. The average velocity of the water is calculated using the time-resolved detector signal. The ultimate purpose is to develop a portable and non-intrusive flowmeter that can be used as a calibration tool.

The objectives of this work were to investigate some parameters that affect the accuracy of the measurement. Both experimental and numerical investigations have been performed.

Developments were made in the transport and mixing of the activity. A Computational Fluid Dynamics (CFD) code was used for the first time in a model of the PNA flowmeter. With the CFD code it was examined how the activity distribution changes with time and its average velocity at different times after the neutron pulse was also calculated. The results showed that there is a substantial discrepancy between the average velocity of the water and the average velocity of the activity. One factor that influences this discrepancy is how the activity is distributed in the pipe directly after the neutron pulse. It is desirable that the initial activity distribution is homogeneous and in this work it was investigated if the homogeneity could be improved. A neutron collimator and an increased distance between the neutron source and the pipe wall were shown to improve the activity distribution in the pipe.

Background radiation is a problem in many nuclear applications and the PNA flowmeter is no exception. The background in a PNA measurement changes both the shape and position of the peak and if not treated correctly it will decrease the accuracy of the flowmeter. A method for identifying the origin of the background as well as a method for subtracting it was developed in this work.

Keywords: Pulsed Neutron Activation, PNA, CFD, Flowmeter, Pipe flow

LIST OF PUBLICATIONS

This thesis is based on the following work in the following papers, referred to by Roman numerals in the text:

I Mattsson, H., Owrang, F., Nordlund, A
Simulation of pulsed neutron activation for determination of water flow in pipes
Kerntechnik, Vol. 67, No. 2-3, pp. 78- , 2002

II Mattsson, H., Nordlund, A., Dahl, B.
Simulation of Pulsed Neutron Activation using a CFD code
CTH-RF-176, 2003

III Mattsson, H., Nordlund, A.
Evaluation of the Pulsed Neutron Activation Method using CFD
Proceedings of PSFVIP-5, Australia, 2005

IV Mattsson, H., Nordlund, A., Dahl B.
Collimation and Background Reduction in the Pulsed Neutron Activation Method for Determination of Water Flow in Pipes
Submitted to International Journal of Nuclear Energy Science and Technology

OTHER PUBLICATIONS BY THE AUTHOR NOT INCLUDED IN THIS THESIS

* Owrang, F., Mattsson, H., Nordlund, A.
A method of water level detection in boiling water reactors using the ^{16}N decay
Kerntechnik, Vol. 67, No. 5-6, pp. 296-298, 2002

* Owrang, F., Mattsson, H., Nordlund, A., Olsson, J., Pedersen, J.
Characterization of Combustion Chamber Deposits from a Gasoline Direct Injection SI Engine
Special SAE paper, SAE-2003-01-0546, 2003

* Owrang, F., Mattsson, H., Olsson, J., Pedersen, J.
Investigation of oxidation of a mineral and a synthetic engine oil
Thermochimica Acta 413/1-2, 241-248, 2003

* Mattsson, H., Nordlund, A.
Remarks on pulsed neutron activation
Kerntechnik Vol. 69, No. 1-2, pp. 66-67, 2004

* Owrang, F., Mattsson, H., Nordlund, A.
A method for in-situ quantification of oxygen in oil using fast neutron activation analysis
Kerntechnik Vol. 69, No. 1-2, pp. 51-57, 2004

* Mattsson, H., Nordlund, A.
CFD Simulation of the Pulsed Neutron Activation Technique for Water Flow Measurements
Proceedings of American Nuclear Society, France 2005

Contents

1. Introduction

1.1. General

Flow measurements of gases and liquids are used in vastly different areas, ranging from individual households to large-scale industrial applications. For example, accurate determination of the environmental impact of a plant requires monitoring of the waste water or emission of gaseous pollutants. In the food and medical industry it is essential to monitor the flow accurately to get a correct composition of the final product and in the water supply industry the amount of water transported to the customers is of interest. In the energy industry the produced energy is frequently transported as thermal energy, often measured with calorimetric methods. As these examples show, the range of measurement situations require highly diversified measurement techniques. Many different types of flowmeters have therefore been developed, each with its characteristics and area of use.

The time it takes for an object to be transported a certain distance in an open stream can be used to calculate the average velocity of the fluid but for pipe flow another approach is required. In pipes, any foreign substance must somehow be introduced through the pipe wall and the substance must be measurable at some distance downstream. The introduced substance can for instance be colour or a radioactive substance. Both these tracer techniques require injection of the substance through the pipe wall which limits the measurement to a certain location of the pipe.

Nuclear measurement techniques are well suited for non-intrusive measurements and the Pulsed Neutron Activation flowmeter (PNA) developed in this work use both neutrons and photons. The neutrons can penetrate the pipe wall and activate the fluid in the pipe while photons emitted from the activity in the pipe can penetrate the pipe wall and be detected by a detector outside the pipe. The difference compared to the tracer measurements is how the activity is introduced into the pipe. The PNA flowmeter requires that the substance in the pipe can be activated by neutrons and that the produced activity emits gamma radiation of a suitable energy. In this work oxygen was used for activation and since this is a fairly common element (e.g. water) this is not a severe limitation. It also emits high-energetic photons that can easily be measured with a gamma detector outside the pipe. The time-resolved signal in one or two detectors downstream from the activation point is used to calculate the average velocity of the water flow.

The principle of the PNA technique is summarised in Figure 1. As can be seen, the procedure can be divided into four stages: activation of the water, transport of the activity, detection of the gamma radiation and analysis of the time spectrum. The outline of this thesis follows this outline, and also includes a section for validation of numerical models against experimental data.

Previous work on PNA (described in more detail in Section 1.2) has shown that it is difficult to extract the flow velocity from the experimental data with a high degree of precision. The aim of this thesis is to improve the understanding of how the different parameters influence PNA measurements, thus improving the accuracy of the method.

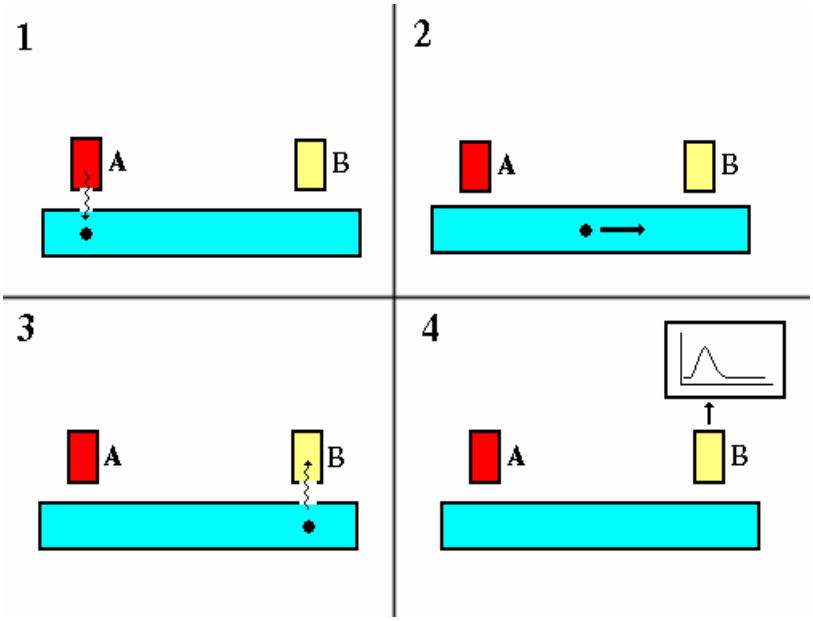

Figure 1: The four stages of a PNA measurement: activation of the water, transport of the activity, detection of the gamma radiation and analysis of the time spectrum. A indicates the neutron generator and B the detector.

1.2. Overview of previous work

Using PNA for determination of the velocity of fluids, solids and slurries was first suggested in 1972 [1]. The two main contributors to PNA have been research groups at ANL (Argonne National Laboratory, Argonne, USA) and RPI (Rensselaer Polytechnic Institute, Troy, USA). Their work was mainly done in the late seventies and early eighties (1976-83). In 1994, a PNA project was started at Chalmers University of Technology. After a feasibility study [2], a number of articles and reports have been published [3-11], including one diploma work [12], three licentiate theses [13,14,15] and one doctoral thesis [16]. The research has progressed along several lines, which may roughly be divided into mathematical models, computer simulations and experimental investigations. As in many other fields, the development of theory and practice has gone hand in hand.

The aim of a PNA measurement is to determine the mass water flow in a pipe from a measured time distribution of gamma radiation at a fixed position on a pipe. The measured time spectrum from a PNA measurement is shown in Figure 2. There are two different ways to determine the velocity of the water by analysing the time spectrum. One way is to determine the average transport time of the activity and calculate the average velocity by using the known distance from the activation point to the detector. A few different averaging methods have been suggested and they are described in some detail below. The other way is to use a computer model of the PNA measurement to evaluate the experimental data.

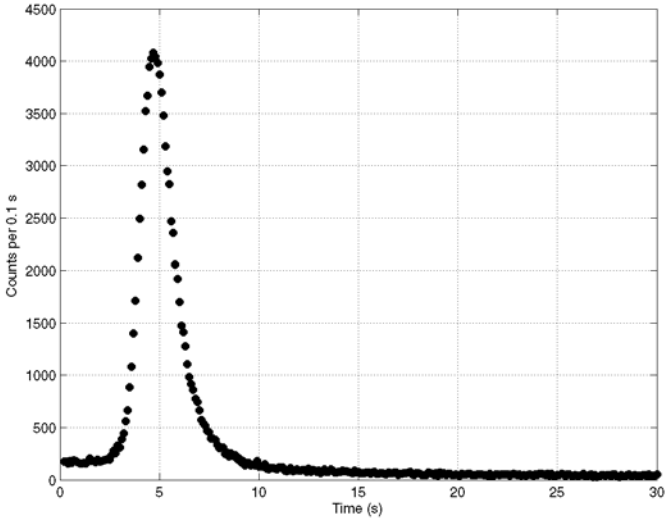

Figure 2: A typical time spectrum from a PNA experiment, showing the signal from the activity passing in front of the detector approximately 5 s after neutron activation.

PNA has also been investigated in fusion power research [17,18,19], where the problem has been the opposite of the one described in this work. Here the velocity of the water is determined, while the fusion problem instead has been to determine the neutron flux. A water pipe passes close to the neutron source and the ^{16}N activity, measured at some point downstream, can be used to determine the neutron flux at the activation point.

Another application of PNA is measuring density variations or void fraction [20-23], which is possible as the induced activity is density-dependent. For example, the effect of air bubbles on the measured time spectrum was demonstrated in [20].

One potential application of the PNA flowmeter is as a way of diversifying flow measurements. The fact that the equipment is non-intrusive and can be made easily movable makes it suitable for validation of the calibration of existing meters and for flow measurements in non-instrumented pipes. It can also be used for intercomparison between meters. The method is mainly suitable for liquids and slurries containing ^{16}O (using the reaction $^{16}O(n,p)^{16}N$). Other possible nuclides have been listed in [1]. For example, the reaction $^{23}Na(n,\alpha)^{20}F$ has been used to measure sodium flow at an experimental breeder reactor [24,25]. The potential to use PNA for gas measurement is limited due to the low density of gas, as the low activity would increase the effect of statistical fluctuations in the signal. Among the advantages of using oxygen, it is worth mentioning the high energy of the photons from ^{16}N (6.1 MeV), which makes the method insensitive to interferences, as the peaks from the ^{16}N can easily be separated from those of other radionuclides. PNA is preferably used for integrated measurements, determining the average velocity of the flow.

2. Experimental equipment

2.1. The piping system

An essential feature of an experimental set-up of PNA is to have a piping system with stable flow. This system was constructed in the initial phase of this project and has been described in earlier works [11, 17]. The piping system consists of a fluid container, a constant fluid level container (CFLC), a weighing tank and a recirculation tank (Figure 3). Between the CFLC and the recirculation tank is the measurement section. This is a long, straight part of the pipe, where the target of the neutron generator and the two detectors are placed. This section of the pipe is in a slightly upward direction to minimise the amount of air bubbles in the pipe. To avoid disturbances, the target of the neutron generator was placed approximately 40 pipe diameters from the closest pipe bend. PVC pipes with an inner diameter of 10.36 cm and wall thickness of 0.4 cm were used.

During a PNA experiment, the water is recirculated to the fluid container after the measurement section. By switching a valve, the water can also be directed into the weighing tank, where the reference mass flow can be determined. The water tank is placed on three piezoelectric scales, one under each leg of the tank. The weight of the water is measured separately with the scales, and the time is measured simultaneously with a quartz crystal timer. The reference flow can in this way be determined with an accuracy of better than 0.5%. The maximum velocity of the flow system is approximately 0.5 m/s [8].

After recirculation through the fluid container, the water flows into the CFLC were the water is kept at constant level through an overflow mechanism. The purpose was to use gravity as the driving force of the flow, making the flow as stable as possible.

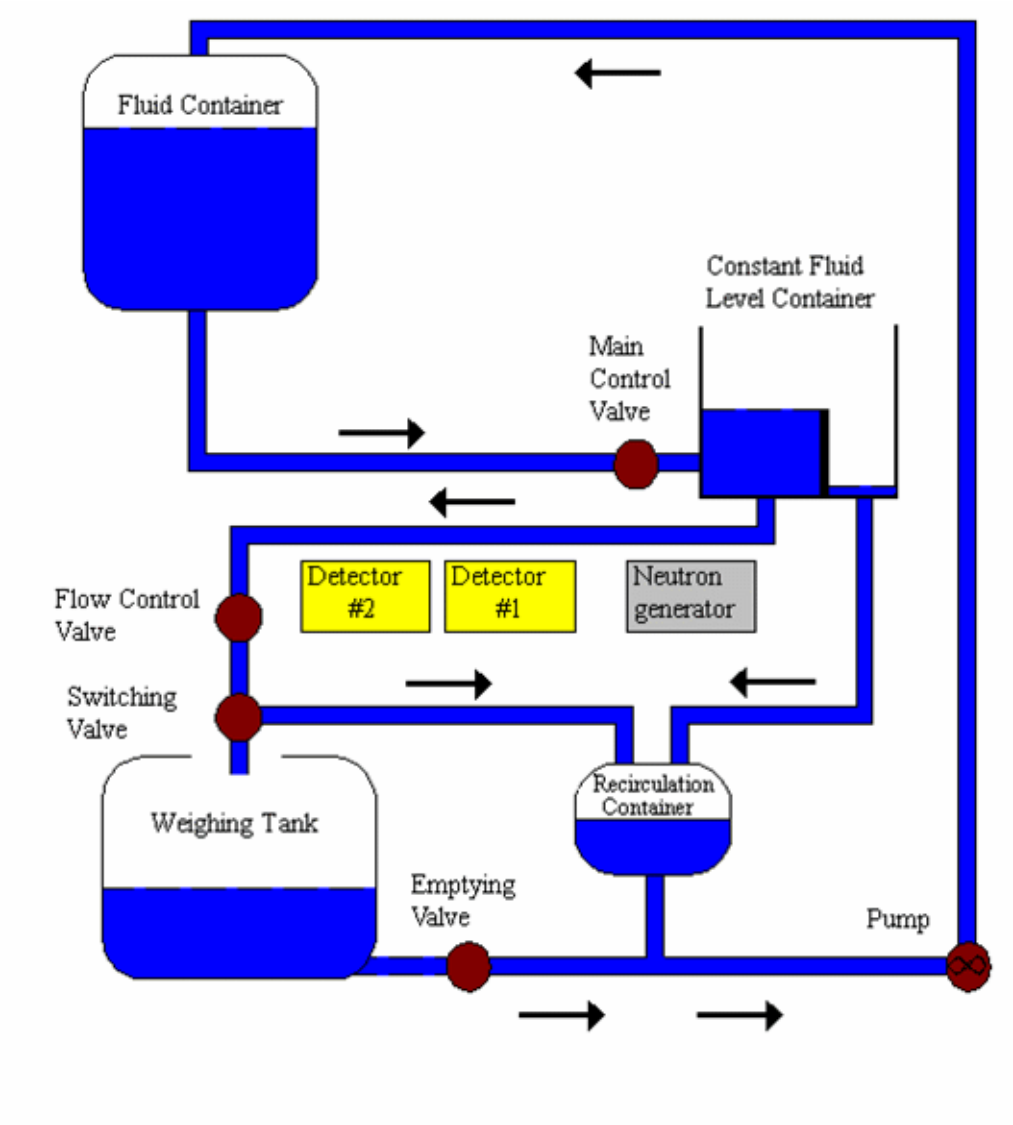

Figure 3: The piping system.

2.2. The neutron generator

The activation of the water in the pipe is achieved by neutron activation of oxygen. The neutrons were produced by a neutron generator (T400, SAMES, France) (Figure 4), where the target of the neutron generator was placed close to the pipe wall.

The neutron generator consists of an ion source, an accelerator tube and a target. Deuterium ions are injected into the accelerator tube and accelerated along the accelerator tube using a 300 kV voltage. The maximum ion current is 1 mA. The $^{3}H(^{2}H,n)^{4}He$ reaction used in this work yields 14.1 MeV neutrons, which are, due to the comparatively low acceleration voltage, emitted almost isotropically. The ion source can be run in either continuous or pulsed mode, where pulse lengths down to 0.01 ms are possible. In this work only the pulsed mode was used, with pulse lengths of 0.1 s. The output of 14.1 MeV neutrons from the neutron generator is up

to approximately 10^{11} n/s, thus approximately 10^{10} neutrons per pulse for a pulse of 0.1 s duration.

One application of PNA is to measure pipe flow at different locations and in this context a stationary neutron generator is not very useful. A portable neutron generator is also available at the Department for use in the PNA project. It works on the same principles as the stationary neutron generator, although the neutron yield is lower, approximately 10^9 n/s. One important difference between the stationary and the portable neutron generator is that with the stationary neutron generator the deuterium beam can be focused so that the neutron source becomes point like. The portable neutron generator does not have such a feature resulting in a more diffuse neutron source.

A cylindrical plastic scintillation (Pilot B) detector with dimensions 2.54×2.54 cm (diameter $\times$ length) was placed above the target of the neutron generator and was used to monitor the output of the neutron generator.

The neutrons from the neutron generator activate the water in the pipe through the $^{16}O(n,p)^{16}N$ reaction, resulting in the radioactive nuclide ^{16}N, which has a half-life of 7.13 s [26]. As it decays, ^{16}N will emit mainly 6.1 MeV (68.8%) and 7.1 MeV (4.7%) photons. The main characteristics of the activation process are summarised in Table 2. For 14 MeV neutrons the cross section is approximately 40 mb [27] and the reaction has a threshold energy of approximately 10 MeV (Figure 5). This relatively high threshold energy reduces the contribution of scattered neutrons to the activation.

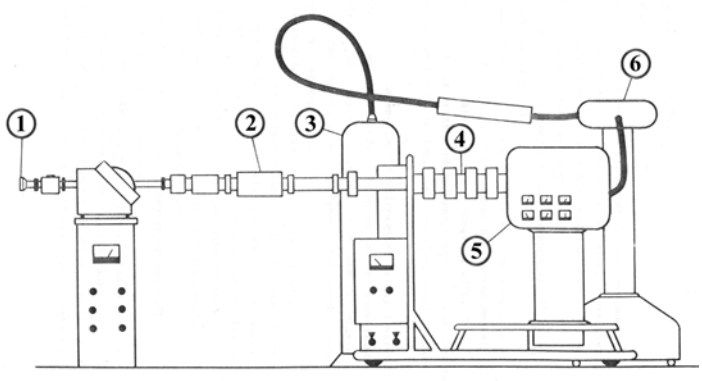

1) Tritium target
2) Travelling wave
3) High voltage generator
4) Accelerating tube
5) Ion source
6) Capacitor

Figure 4: The stationary neutron generator.

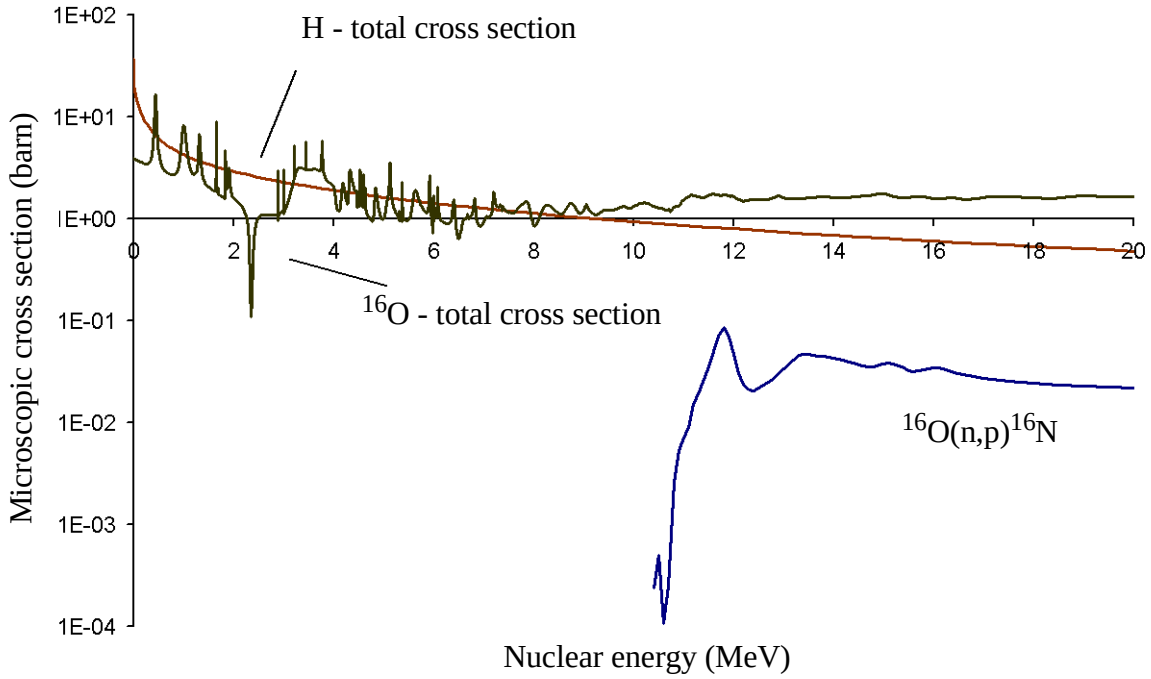

Figure 5: Cross section of the $^{16}O(n,p)^{16}N$ reaction compared to the total cross section of hydrogen and oxygen. Data from [28].

Table 1: Nuclear data of ^{16}N and the $^{16}O(n,p)^{16}N$ reaction.

Gamma energies [26]	1.755 (0.10%) 2.741 (0.89%) 6.129 (68.8%) 7.115 (4.7%)
Half-life [26]	7.13 s
Threshold energy for the (n,p) reaction [27]	~10 MeV
Cross section at 14 MeV [27]	~40 mb

2.3. The detectors

Due to the high energy of the photons from ^{16}N (6.1 MeV), the measurements demand a detector with high efficiency. Two cylindrical 5.08×5.08 cm (height $\times$ diameter) BGO scintillation detectors (Teledyne Brown Engineering, USA) were used. The high density of BGO (7.3 g/cm^3) and its high atomic number (83) results in the highest probability for the photoelectric effect per cm^3 of any commercially available scintillator [29]. On the other hand, due to its low light yield the resolution it not very high. In this application the importance of efficiency is much greater than that of energy resolution.

A collimator covering the whole length of the detector was used. Its purpose was to minimise radiation coming from ^{16}N in the pipe upstream and downstream of the detector position. This is important, since the purpose of the measurement is to determine the transport time from the neutron source to the detector. The collimator consists of a cylindrical collimator (2.3 cm of lead and 0.3 cm of aluminium). This collimator stops approximately 70% of the 6 MeV photons arriving perpendicular to the collimator.

The detectors could be used for two types of measurements: time measurements (Figure 6) and energy measurements. Time measurements, used for the determination of the water flow, are the primary interest in this work but some applications of energy measurements have also been found. In both cases each detector was connected to a linear amplifier. In the time measurements, the signal from the amplifier was connected to a MCS unit and to a PC. In the energy measurements, the signal was connected to an MCA and then to a PC.

In the time measurement set-up, the variation of the signal in time in a specified energy interval was studied. The level of the lower threshold is the most critical and its selection is a trade-off between including as much of the signal as possible and as little of the background as possible. A level of 4 MeV was chosen, which is in accordance with earlier results [16]. The upper threshold is not so critical as the background is very low and there are no interfering peaks from other sources in that region. The upper threshold was set to 10 MeV in this work.

To determine the average transport time of the activity correctly, it is important that both detectors start measuring at a well defined time, in our case the time of the neutron pulse. This is achieved by sending a trigger signal from one of the MCS units to the neutron generator and the other MCS unit simultaneously.

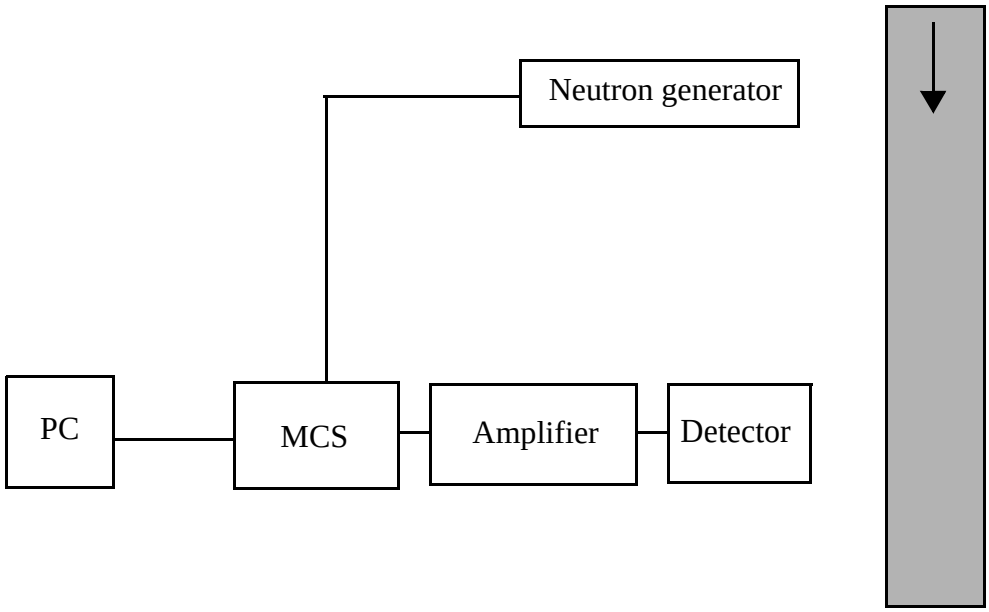

Figure 6: Detector set-up for time measurement.

3. Part I: Activation

3.1. General

In most works on PNA, as well as in the experiments described in this work, the target of the neutron generator was placed close to the pipe wall in order to maximise the activity in the pipe. This will lead to a high gradient of the neutron flux in the pipe and subsequently to a high gradient of the induced activity concentration in the pipe. With this set-up, there will be a high concentration of activity close to the pipe wall where the velocity of the water is low due to the velocity profile in the pipe. The initial average velocity of the activity will subsequently be lower than the area-average velocity of the water and the activity will not have reached a homogeneous radial distribution even when it passes the detector, as will be discussed in more detail below. It would therefore be desirable if the velocity of the activity, which is the measured quantity, would be more representative of the water flow, which is the desired quantity. Moreover, if the initial activity was more homogeneous, the subsequent mixing of the activity might be described by some theoretical model, e.g. [30]. These aspects were investigated in Paper III and IV.

The spatial distribution of the activity in the pipe will depend on the experimental set-up, such as the distance between the neutron source and the pipe wall, and the pipe diameter. Previous work has shown that the initial activity is indeed inhomogeneously distributed. For example, it has been shown that for a pipe diameter of 10 cm, about 50% of the activity is within 1 cm from the wall [15]. In order to deal with this, several authors have tried to improve the initial activity distribution, so that it becomes more homogeneous. One attempt was to use four neutron generators emitting neutron pulses simultaneously to achieve a more homogeneous activity distribution [31]. Although it was shown that an improved activity distribution could be achieved, this does not seem to be a practical solution. Another, cheaper, solution is to use a collimator to decrease the activity upstream and downstream from the neutron source. Experiments have shown that using a collimator did change the shape of the measured time spectrum [5]. In using a collimator it was also hoped that the activity distribution would become more localized, which would make the velocity of the activity more representative of the flow. A more homogeneous activity distribution might also make it possible to apply some theoretical expression for description of the mixing of the activity could be applied. One such expression that has been used as an approximation in PNA [8] was derived by Taylor [30, 32]. However, Taylor's expression is based on the assumption that the activity is initially confined to an infinitely thin slice in the pipe.

3.2. Results

3.2.1. Effect of a collimator

Further investigations of the effect of a collimator and the distance between the neutron source and the pipe wall were performed and reported in Paper IV (Figure 7). Four different collimator materials (Fe, W, Pb and C) were investigated in the study and the axial and radial activity distribution was compared to the distribution when no collimator was used. Three different source-wall distances (1, 3 and 10 cm) were also tested. It was found that tungsten was the best collimator material of the four materials tested but in order to achieve a substantial effect, the source-wall distance should be increased to 10 cm. This set-up would decrease the

activity in the pipe upstream and downstream from the neutron source and it would also make the activity more homogeneous in the radial direction. These are both desired effects but the increased distance cause the total amount of activity in the pipe to decrease which will increase the measurement time or worsen the counting statistics.

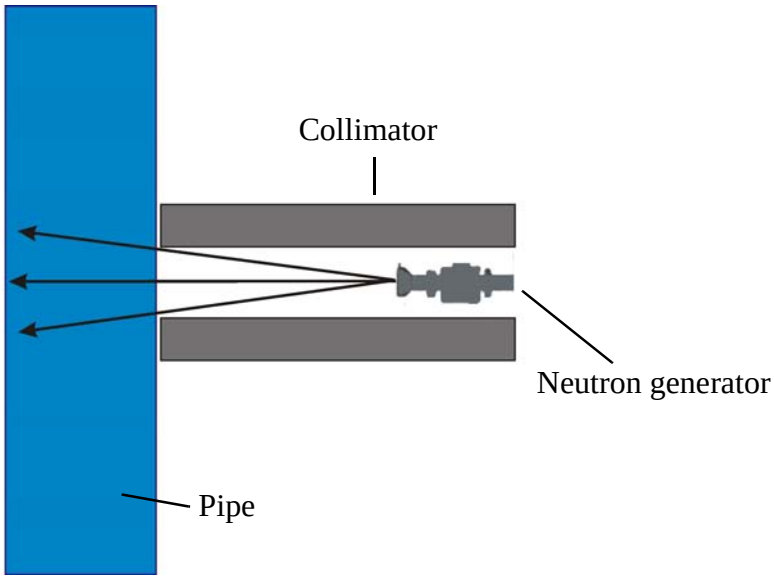

Figure 7: Set-up of a collimator.

The conclusion from the investigations of using a collimator was that even though an improved activity distribution could be achieved, the gradient was not sufficiently reduced to motivate the loss in activity due to the increased source-wall distance. No theoretical model like Taylor's does therefore apply and computer simulations of the activation and transport are probably necessary. In that case, including a collimator in the experimental set-up would only introduce one more factor to take into account.

3.2.2. Effect of the initial activity distribution

Another aspect of the initial activity distribution was discussed in Paper III. In this work, the initial conditions for the Computational Fluid Dynamics (CFD) calculations were investigated. Activity starting in different parts of the pipe will not contribute equally to the detector signal. The relative contribution to the detector signal from different parts of the initial activity distribution was investigated.

The 2D pipe in Paper III was divided into eight different volumes limited by concentric circles 1 cm apart (Figure 8). Activity was distributed in each of the eight volumes separately and its impact on the detector signal was studied (Figure 9). The detector signal was calculated using the response function described in more detail below (Section 5). As the neutron source can be approximated with a point source 1 cm from the edge of the pipe wall, the activity in the pipe decreases rapidly with the distance from the source. The contribution from the different volumes to the detector signal is shown in Figure 9 (A1-A8). It can be seen that activity originating from volume 1 contribute the most to the detector signal and that the contribution from the other volumes decreases with decreasing distance from the neutron source. Thus, it

can be concluded that the initial activity distribution can not be approximated with only one small volume close to the pipe wall but that the region around the neutron source should also be included, although it is possible that the high gradient of the activity should be resolved further.

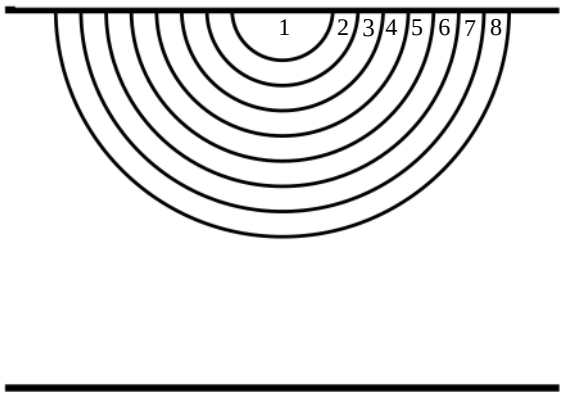

Figure 8: Division of the pipe into eight smaller volumes for investigation of the initial activity distribution on the detector signal.

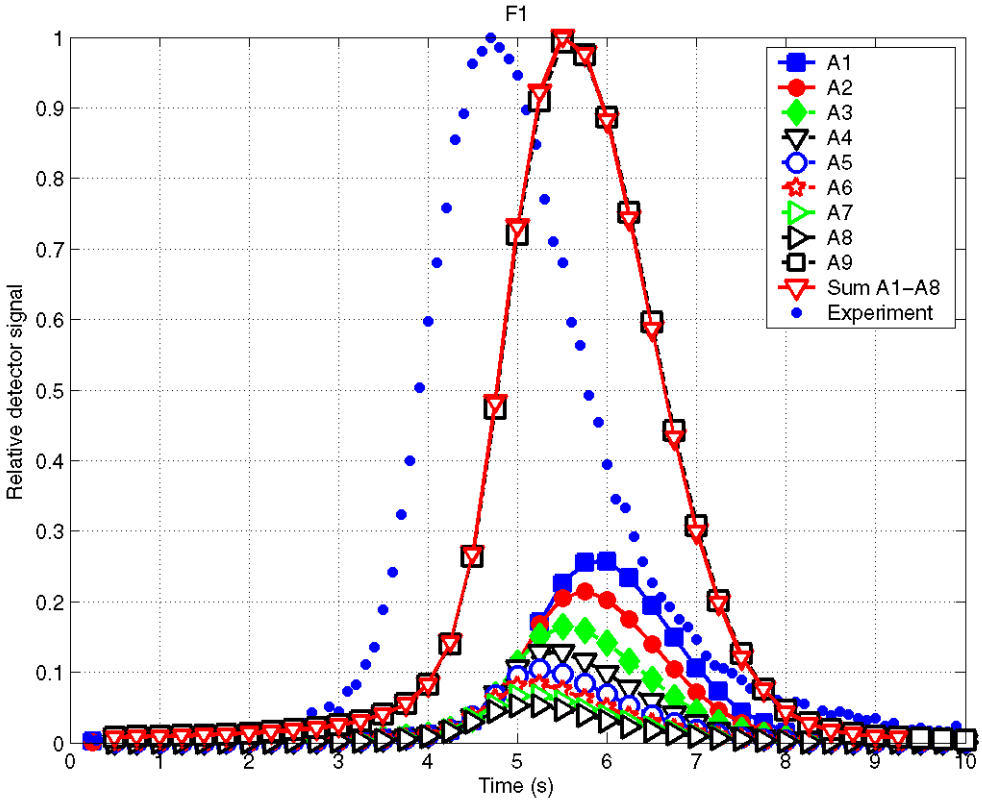

Figure 9: The calculated detector signal from different initial activity distributions compared to experimental data. A1-A8 denotes activity starting in volume 1-8, respectively. A9 denotes a weighted activity distribution starting in volumes 1-8 simultaneously. For details see Paper III.

4. Part II: Transport and mixing

After having calculated the initial activity distribution, the subsequent transport of the activity in the pipe must be calculated. The PNA flowmeter is thought to work best for fully developed, turbulent flow because of the improved mixing of the activity in the water. In this section the basics in fluid dynamics is summarised, with the emphasis on turbulent pipe flow, since all experiments in this work were conducted with turbulent flow [33, 34].

4.1. Fluid dynamics and numerical modelling

4.1.1. General

Fluid flow can be divided into mainly two groups, laminar and turbulent flow. Laminar flow where the flow velocity is low is characterised by a predictable motion of the water. For a fixed point in the pipe, the speed of the water is time-independent. The water also travels along well-defined paths and fluid elements starting at the same point follows the same path. If the velocity of the water is increased, the flow will at some velocity begin to develop a random character with rapid, irregular fluctuations in time and space. Elements starting at the same position in the pipe will follow different paths, since the irregularities are changing all the time. This latter flow is called turbulent. In turbulent flow both the magnitude and direction of the flow varies rapidly in time.

In fluid dynamics, the Reynolds number (Re) is a dimensionless parameter used to define the flow pattern. For pipe flow, it is defined by

$$Re = \frac{\rho u d}{\mu} \qquad \text{Eq. 1}$$

where ρ is the density of the fluid, u is the average velocity of the fluid, d is the pipe diameter and μ is the dynamic viscosity. The value of the Reynolds number can be used to determine the flow regime of the flow. The transition from laminar to turbulent flow is usually set to Re=2300.

4.1.2. Velocity profile, boundary layer and fluid mixing

Water entering a pipe from a tank initially has a flat velocity profile, i.e. the velocity of the water is independent of the distance from the pipe wall. However, the water close to the pipe wall is retarded and subsequently the water in the middle of the pipe must accelerate to maintain the mass flow. In this way a velocity profile will develop with the highest velocity in the middle of the pipe and lowest at the edges. This will continue until the flow is fully developed, i.e. when the shape of the velocity profile no longer changes. The velocity profile in a pipe differs for laminar and turbulent flow in that the turbulent flow profile is much flatter (Figure 10).

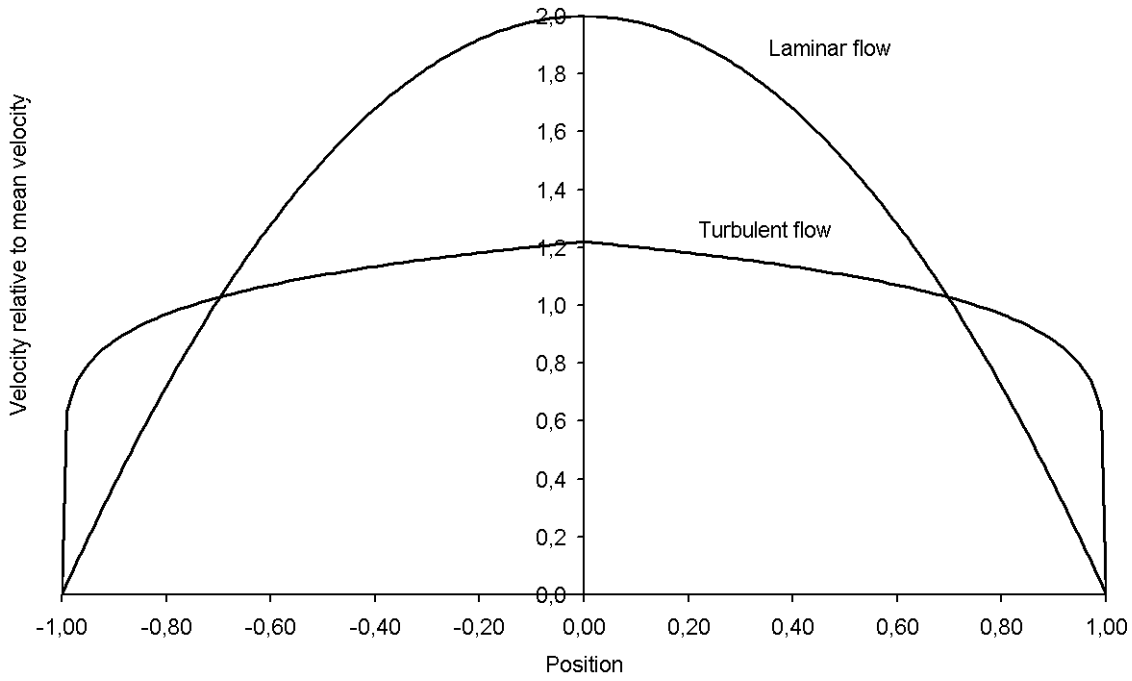

Figure 10: The velocity profile in laminar and turbulent flow in a pipe.

The concept of a boundary layer is important in many aspects of fluid flow and it is also important in PNA. It can easiest be understood by considering fluid flow over a plate. At a large distance from the plate, the influence of the plate is negligible and the velocity is constant (free-stream velocity). Moving closer to the plate, the velocity decreases due to the viscous forces of the fluid until it becomes zero at the surface. Thus, the velocity of the fluid depends on the distance from the plate (velocity profile). The boundary layer is defined as the region closest to the plate where the velocity is less than a certain fraction of the free-stream velocity, for example 99%. As there is no distance where the plate has no effect, the thickness of the boundary layer can be chosen arbitrarily.

Mixing in a pipe is a result of two forces, molecular diffusion and by transfer through eddy currents. The boundary layer can be divided into three layers depending on which force dominates the mixing. The three layers are called the sub-laminar layer, the buffer layer and the turbulent boundary layer. In the sub-laminar layer close to the pipe wall, the only motions perpendicular to the surface are due to molecular diffusion. In the intermediate buffer layer, molecular diffusion and eddy motion are of comparable magnitude while in the turbulent boundary layer, most distant from the wall, the eddy motion is large compared to molecular diffusion. In a pipe, the thickness of the laminar sub-layer (δ_b) can be defined by [33]

$$\frac{\delta_b}{d} = 62 \cdot Re^{-7/8} \qquad \text{Eq. 2}$$

where d is the diameter of the pipe and Re is Reynolds number. The sub-laminar layer is not a completely discrete region as it has been shown that from time to time eddies penetrate into the sub-laminar layer [33].

4.1.3. Governing equations and numerical modelling

The governing principles of fluid flow are that the mass of the fluid is conserved (continuity equation), that the rate of change of momentum on a fluid particle equals the sum of forces (Navier-Stokes equation/Newton's second law of motion) and that total energy is conserved. These equations form the basis for all flow calculations. However, the governing equations are impossible to solve analytically for turbulent flow except for very simple geometries and flow conditions. For more complicated geometries a numerical solution can be obtained by solving the discretized version of the governing equations.

Several numerical solvers exist and in this work the CFD solver Fluent [35] was used for obtaining a numerical solution for the transport and mixing of the activity in the pipe. The standard kε-model was used for the calculations in this work and the average velocity from the experiments was used as boundary condition on the inlet. The grid was generated in Gambit and the length of the pipe upstream from the neutron source was long enough to allow for fully developed flow.

4.1.4. Dispersion of a tracer in a pipe

A theoretical description of the dispersion of a tracer in a pipe for both laminar and turbulent fluid flow has been made by Taylor [30,32]. In his calculations, it was assumed that the substance distribution initially is homogeneously concentrated in an infinitely thin plane perpendicular to the pipe axis. An expression was derived that describes how the concentration at a certain distance downstream varies with time.

$$C(z,t) = \frac{A}{\sqrt{\pi K t}} \cdot \exp\left[\frac{(z-\bar{u}t)^2}{4Kt}\right] \qquad \text{Eq. 3}$$

C(z,t) is the mean concentration of activity at axial position z and at time t, $\bar{u}$ is the mean velocity of the water and K is the virtual coefficient of diffusion. The value of K depends on whether the flow is laminar or turbulent. A is the initial number of particles per unit area. This expression was derived for large distances, more than 50 pipe diameters from the starting point.

The shape of the distribution for some different values of z is shown in Figure 11. There are two main features in the curve. One is that the amplitude of the curve decreases as the distribution becomes more and more elongated for large values of z. The other is that the distribution is asymmetric around the maximum with a main group of particles followed by a long tail.

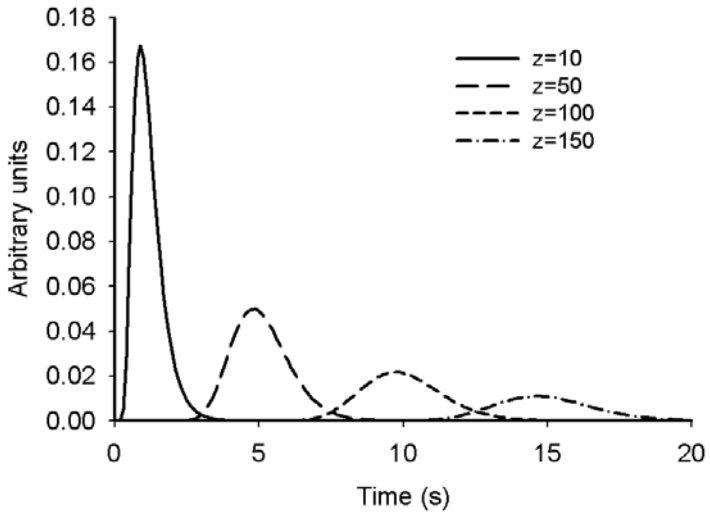

Figure 11: Taylor distribution (Eq. 3) for different values of z. ($\bar{u}$=10, K=10, A=1).

4.2. Results

4.2.1. Colour experiments

It has previously been known that the activity in the pipe is inhomogeneously distributed, both directly after the neutron pulse and when it passes the detector. However, it has not been known to what extent this affects the measurements and if it is necessary to take it into account when evaluating the measurement. An experimental study of the inhomogeneity of the activity when it passes the detector was made in Paper I.

Colour, simulating the activity, was inserted close to the wall of a transparent Plexiglas pipe, which had the same inner diameter as the pipes used in the PNA experiments. The colour distribution was recorded with a video camera at three different positions downstream. Results showed that the colour was not very well mixed with the water in the investigated part of the pipe.

The experiment showed that the velocity of the activity in a PNA experiment did not have the same velocity as the water when passing the detector. As the measured quantity in a PNA experiment is the velocity of the activity it seemed a highly relevant question to determine how much the two velocities differ. From the colour experiments, an estimation of the velocity of the colour was done where the radial colour distribution was combined with an assumed velocity profile of the water. A velocity of the colour could then be calculated and it was found to be initially approximately 10% lower than the average velocity of the water and then increasing as it was transported downstream.

The conclusion drawn from the colour experiments was that it was indeed necessary to simulate the transport of the activity in the PNA measurement in order to accurately model the water velocity.

4.2.2. CFD

In a pilot study (Paper II), the CFD solver Fluent 6.1.22 was used to simulate the transport and mixing of the activity in the pipe in 3D. In this study, the initial activity distribution could be better approximated than in the colour experiments described above, since the initial activity distribution was calculated using Monte Carlo calculations. The transport and mixing of the activity downstream in the pipe was studied. Since there was no detector response function available, the detector signal was not calculated in this study and the results are therefore more qualitative. The activity distribution was calculated in a cross-section of the pipe at different times and the results give a good illustration of the behaviour of the activity. Improvements on the initial conditions for the calculations can be made since the present geometry does not fully resolve the high gradient of the activity distribution close to the neutron source.

Another CFD calculation is presented in Paper III. In this work, a 2D model of a pipe was simulated. As it was not straightforward to use the Monte Carlo calculations in the 2D case, the neutron source was approximated with a point, emitting neutrons isotropically and the activity concentration could be assumed to follow the inverse-square law. The inverse-square law is a good approximation as there is no need to take the scattered neutrons into account since there is a threshold energy for the $^{16}O(n,p)^{16}N$ reaction at about 10 MeV. In addition, the relatively low cross section of the reactions makes self-shielding negligible. Also, the point-like nature of the neutron source is a good approximation as the beam of deuterium ions that hits the tritium target is very narrow. The activity in the pipe was calculated in concentric circles of 1 cm thickness (Figure 8). As was discussed above, it is important to know how much the average velocity of the activity differs from the velocity of the water. This was calculated from the CFD data and it was found that the average velocity of the activity initially was 7% lower than the average velocity of the water for a water velocity of 19 cm/s (Figure 12). This should be compared to the 10% discrepancy calculated from the data of the colour experiments.

The velocity will then increase rapidly as the activity will mix with the water in the pipe and will approach the velocity of the water. Since the velocity profile is relatively flat in the middle of the pipe, the average velocity of the activity will approach the average velocity of the water relatively fast. Although the velocities are the same, the activity will not be homogeneously distributed in the pipe.

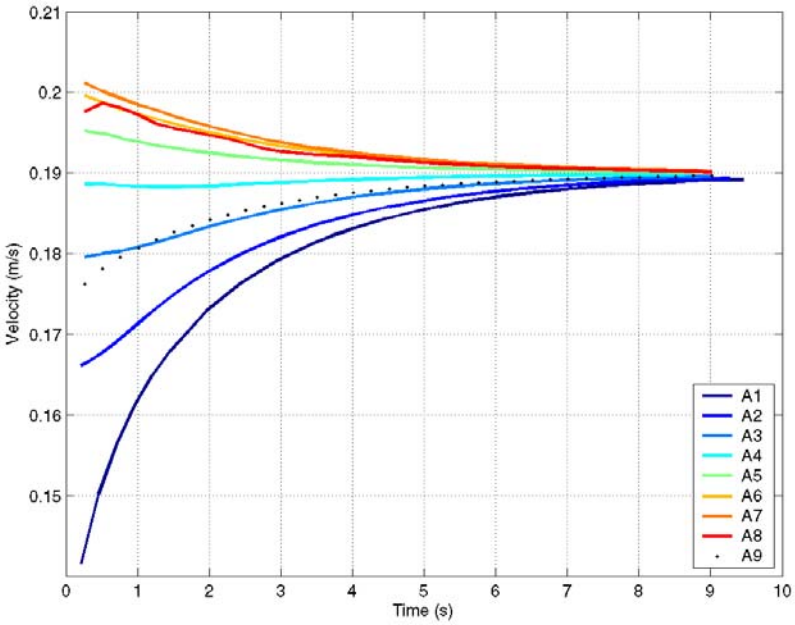

Figure 12: Velocity of the activity at different times after the neutron pulse for activity starting in different volumes. A1-A8 denotes activity starting in volume 1-8, respectively. A9 denotes a weighted activity distribution starting in volume 1-8 simultaneously. For details see Paper III.

5. Part III: Detection

5.1. General

In order to calculate the time resolved detector signal, the simulated activity distributions from the CFD calculations must be used in combination with a detector response function. This response function simply models the detector dependence on the position of the activity.

5.2. Results

5.2.1. The response function

In Paper III, the response function of the detector was calculated using Monte Carlo calculations. The set-up for the calculations is shown in Figure 13. The pipe was divided radially into 13 volumes (not shown in the figure) and axially into eight slabs, each with a thickness of 2.5 cm. Activity of ^{16}N was distributed in the volumes one by one and photons emitted from the activity which interacted in the active part of the BGO detector were registered as counts in the detector. Due to symmetry (upstream/downstream and upper/lower half of the pipe) only a quarter of the pipe had to be calculated. The attenuation and build-up of photons in the water was ignored as this effect is comparatively small. The response function has been compared to what would be measured by a point detector placed 1 cm from the edge of the pipe following the inverse-square law.

The results from the calculations are shown in Figure 14 and 15. A good agreement between the two response functions is seen in Figure 14 where the average of the response function is calculated in each slab. However, this does not take the steep gradient of the response function close to the detector into account. A radial comparison between the two response functions is shown in Figure 15. Here it can be seen that the two functions differ mainly in regions where the effect of the collimator is large. This is at the sides of the detector, close to the pipe wall, and activity in this region will be overestimated using the inverse-square law.

Thus, the inverse-square law is a reasonably good approximation of the response function although it does not cover all the features seen in the Monte Carlo calculations. This is attractive since the response of the point detector can be applied more easily to the results from the CFD calculations without knowledge of exact geometries.

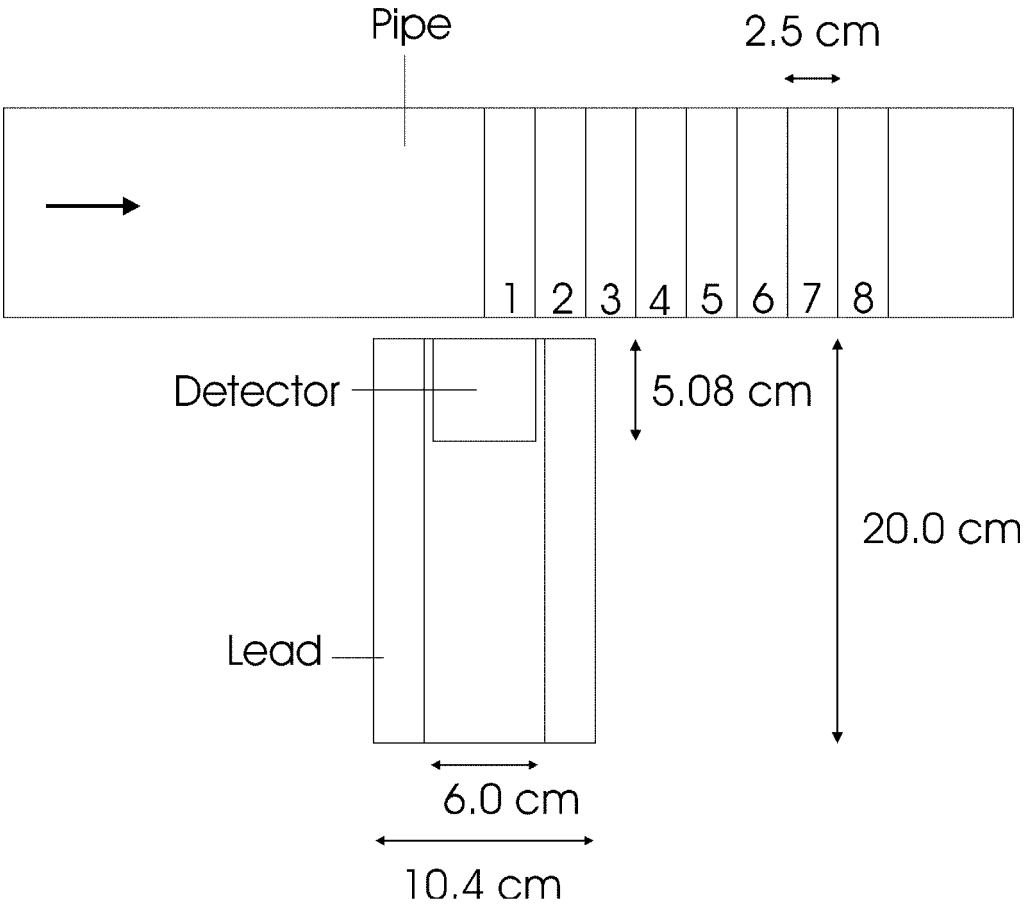

Figure 13: The set-up for the calculation of the response function.

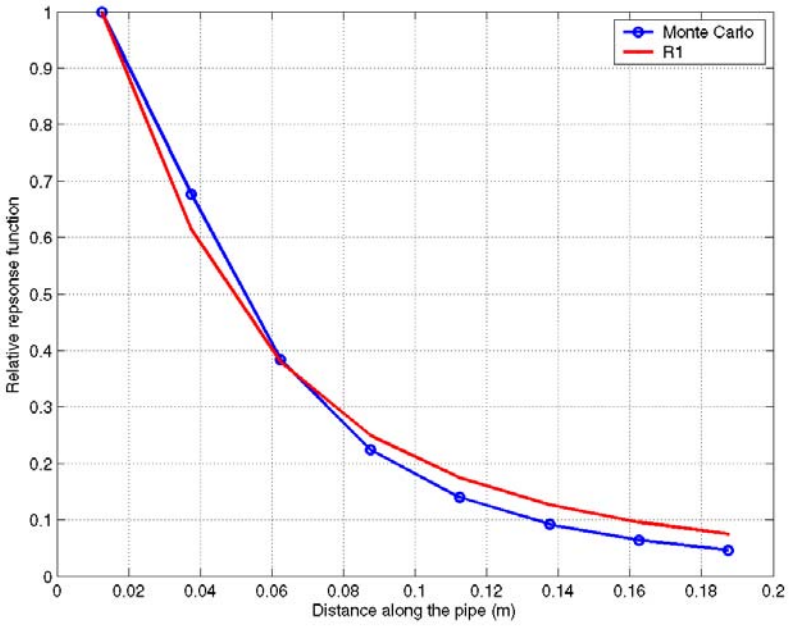

Figure 14: The response function calculated using Monte Carlo calculations and the inverse-square law.

5.2.2. The detector position

The effect of the position of the detector was discussed in Paper III. Both experiments and simulations have shown that a detector placed on the same side as the neutron source will measure a shifted time spectrum compared to a detector placed on the opposite side. This is an effect of the inhomogeneous activity distribution and must be considered when evaluation of the time spectra from a PNA measurement is made.

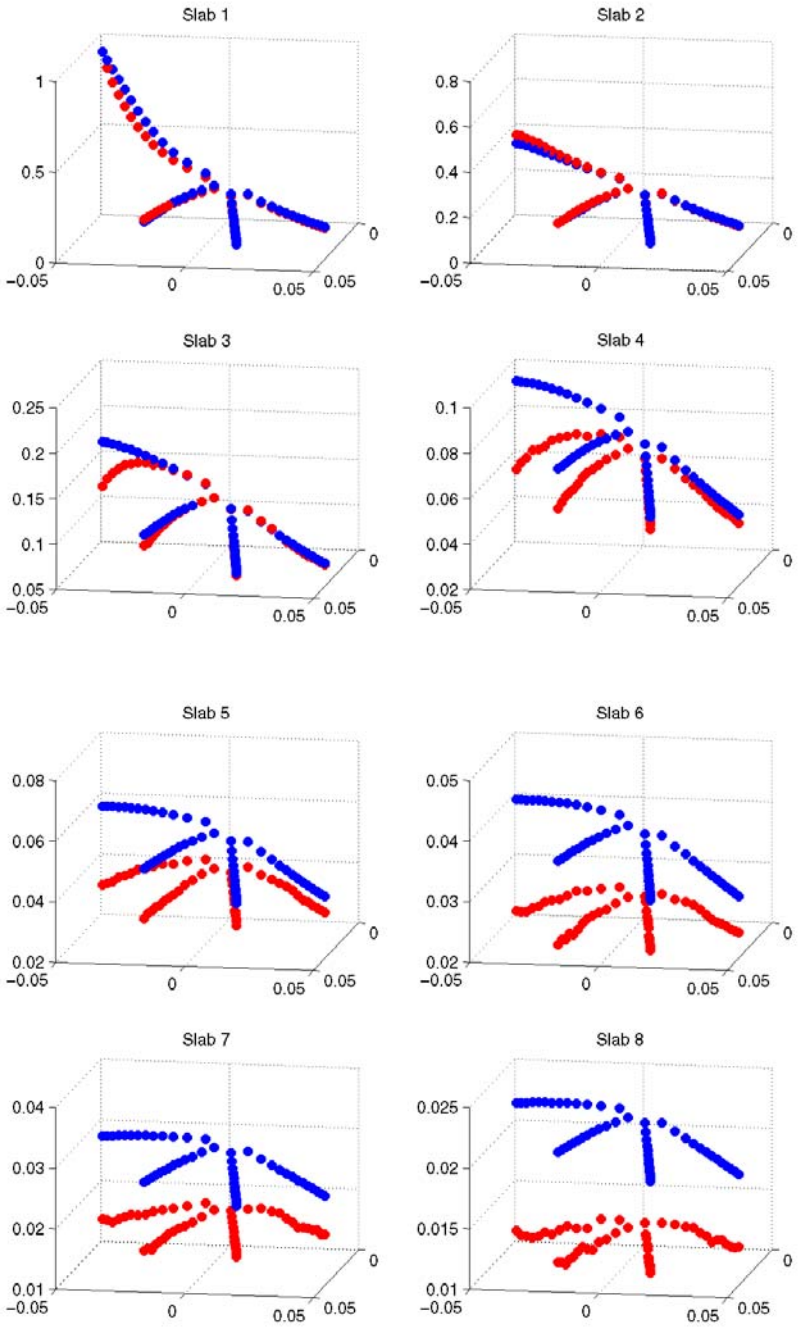

Figure 15: A radial comparison between the response function calculated with Monte Carlo (red) and the response function from a point detector (blue) in eight different slabs at different axial distances from the neutron source.

6. Part IV: Evaluation

6.1. Evaluation methods

Determination of the flow velocity from experimental data can be done in several different ways. The evaluation methods found in literature can be divided into two main groups, averaging methods (Method I) and numerical methods (Method II). The advantage with the averaging methods is that they are fast and simple, but on the other hand they are not very accurate as they do not take into account that the velocity of the activity differ from the activity of the water. The numerical models can be more accurate but are more complicated to use, since they require simulated data to compare the experimental data with. The methods are described below.

6.1.1. Evaluation method I: Averaging

6.1.1.1. Averaging equations

The different averaging methods suggested in the literature are shown in Equation 1-3. C_i is the number of pulses in time channel i, λ is the decay constant and t is time.

$$\left\langle \frac{1}{t} \right\rangle = \frac{\sum_{i=1}^{N} \frac{C_i \cdot \exp(\lambda t_i)}{t_i}}{\sum_{i=1}^{N} C_i \cdot \exp(\lambda t_i)} \qquad \text{Eq. 4}$$

$$\left\langle \frac{1}{t^2} \right\rangle = \frac{\sum_{i=1}^{N} \frac{C_i \cdot \exp(\lambda t_i)}{t^2{}_i}}{\sum_{i=1}^{N} \frac{C_i \cdot \exp(\lambda t_i)}{t_i}} \qquad \text{Eq. 5}$$

$$\langle t \rangle = \frac{\sum_{i=1}^{N} C_i t \cdot \exp(\lambda t_i)}{\sum_{i=1}^{N} C_i \cdot \exp(\lambda t_i)} \qquad \text{Eq. 6}$$

From the above equations, the average velocity of the activity is calculated as L<1/t>, L<1/t^2> and L/<t>, respectively, where L is the distance between the neutron source and the detector.

Both the flow regime (laminar/turbulent) and the distance from the neutron source have been suggested to influence the choice of average method [8,25,31]. For example, some authors recommend the $<1/t^2>$ averaging method for turbulent flow [36], while others recommend the $<1/t>$ equation for turbulent flow and the $<1/t^2>$ equation for laminar flow [31]. It has also been reported that for short distances between the neutron source and the detector, the $<1/t>$ equation was better than the $<1/t^2>$ equation while for larger distances the two were reported to be equal [25]. A comparison between the $<t>$ and the $<1/t>$ equations showed that the $<1/t>$ equation gave a better estimate of the mean velocity [8]. However, none of the investigated averaging methods were found to be completely satisfactory, as pointed out in e.g. [31].

6.1.1.2. Peak value

One simple method for evaluating PNA data is to use the time difference between the peaks of the time distributions, measured with two detectors at different distances downstream from the activation point. This was tried in a feasibility study as a rough estimate of the time [4]. The reproducibility was good but the flow velocity was shown to be much too low compared to the reference flow.

6.1.1.3. Cross-correlation

An attempt to measure the velocity of the activity with cross-correlation was made in [12]. Three neutron pulses shortly after each other were used to activate the water. The three peaks in the time-resolved detector signal (instead of one) were subsequently used to determine the velocity of the water using cross-correlation. The results were not encouraging as the velocity determined was 20% higher than the reference flow.

6.1.1.4. Conclusions: time averaging

Although attractively simple, there are several disadvantages with the time averaging methods. One is that they do not take into account that the average velocity of the activity differs from the velocity of the water in the pipe. It has been shown in this work that this is an effect that must be taken into account. Another disadvantage is that these methods do not take the response function of the detector into account. Finally, the equations were developed assuming an idealised initial activity distribution which does not apply in the experimental situation.

6.1.2. Evaluation method II: Numerical models

Since time averaging methods seem to be insufficient to evaluate the experimental data other methods have been investigated. A more accurate modelling of the PNA experiments would make it possible to simulate time spectra for the geometry present in the experimental set-up. If a set of simulated data for different velocities is available, the unknown velocity in the experiment can be deduced by comparing the experimental and simulated data. One suggested method for the comparison is to use neural networks [3]. This method obviously requires a model of the PNA measurement so that simulated time-spectra can be produced. Several different models have been developed using numerical simulations [3,31,37]. This is also the approach used in this work, where CFD calculations are used in combination with calculations of the initial activity distribution and a detector response function.

6.2. Results

6.2.1. Background subtraction

It has been known for a long time that there is a time-dependent background distribution in a PNA experiment that does not originate from ^{16}N moving with the water. This is important, as it will influence the shape of the peak as well as shift its position in the time spectrum making an accurate comparison with experimental data impossible. Despite the importance of the background, there has not been an appropriate method to correct for the background. Different methods have been used: the linear subtraction method [3,5,8,16,31,38], where a straight line has been drawn from the left to the right side of the peak or one [5,6] or two exponential [25] functions. A general method for identifying and subtracting the background was developed in Paper IV.

In this work, two detectors were used to identify the background. One was placed at a certain distance upstream from the neutron source and another downstream at the same distance. If the distance is large enough, the upstream detector will only measure stationary activity in the surrounding and the downstream detector will measure stationary activity in the background plus the activity moving in the pipe. The distance chosen depends on the initial length of the activity in the axial direction. In Paper IV, it was shown that 30 cm from the neutron source, the activity concentration is less than 1% compared to the activity concentration in front of the neutron source. Hence, the axial length of the activity is approximately 60 cm, 30 cm in each direction. The axial length of the activity will depend on the experimental set-up, like pipe diameter and source-wall distance. The results from this work showed that the upstream detector measured a single exponential which was shown to originate from stationary ^{16}N in the surroundings (Figure 16). It was also found that there is a background component which is time-independent during the measurement.

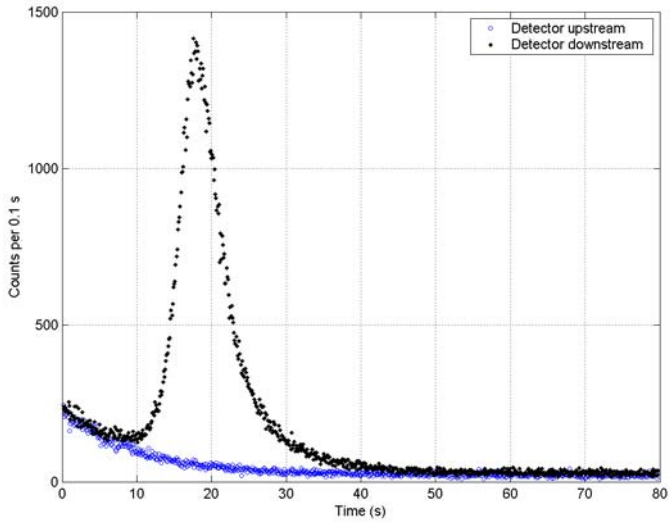

Figure 16: Detector signals measured with a detector upstream and downstream from the neutron source.

After the components of the background have been identified it is in most cases a simple task to subtract it from the time spectrum. However, curve-fitting of the background can be difficult in some situations, for example when the transport time of the activity is short and curve-fitting can only be made on one side of the peak. In Paper IV, an equation for fitting the peak was developed. This could be used together with the expression for the background to separate the peak from the background. No single expression has been found that fits the peak in a PNA time spectrum, but both a Taylor distribution and a Gaussian distribution has been used as first-order approximations [8,25]. None of these expressions were found to fit the PNA data in this work and a sum of several Taylor distributions were used to fit the peak and a good fit was achieved for the cases tested. It should be pointed out that the Taylor distributions are merely an empirical way to describe the shape of the peak and thus do not have a physical meaning in this context but only serve to subtract the background.

7. Part V: Validation

Before a numerical model of PNA can be used to evaluate experimental data, validation or benchmarking of the model must be made. This is done by simulating data with a known velocity. Only a few articles on validation of PNA models are known from the literature [3,31,37] and only [3] was judged suitable of evaluating the accuracy of the model.

As has been described above, a PNA model has been developed in this work. Models of activation, transport and detection have made it possible to calculate a time spectrum for a known water flow which can be compared to experimental data with a known, reference velocity. The results from the model in Paper III is shown in Figure 9 where it can be seen that the simulated curve (A9) and the experimental curve have the same shape and width but the curves are shifted in relation to each other. The simulated curve is shifted to the right, indicating a longer transport time.

As the present model was made in 2D, a direct comparison between simulated and experimental data can be misleading. However, an estimation of how much a change from 2D to 3D affects the position of the time spectrum can be done by applying the correction factor in Eq. 7. This correction factor uses the fact that the shape of the 2D and 3D profiles are similar, which means that the average velocity in 2D can be scaled so that the 3D velocity profile is achieved in the 2D geometry:

$$k = \frac{\int u_{3D}(r)dA_{2D}}{\int dA_{2D}} \cdot \left[\frac{\int u_{2D}(r)dA_{2D}}{\int dA_{2D}}\right]^{-1} \cdot k_{err} \qquad \text{Eq. 7}$$

Here u_{2D} and u_{3D} are the velocity profiles and k_{err} corrects for that the fact that the average velocities in the simulations and in the experiments were slightly different (~4%). Using the calculated velocity profiles it could be shown that the profile for 0.19 m/s in a pipe could be achieved in a channel by increasing the average velocity about 10%. The position of the peak can now be corrected for the geometrical effect

$$\Delta t = kt_{peak} \qquad \text{Eq. 8}$$

The time shifted spectrum is shown in Figure 17. It can be seen that the geometrical effect accounts for a large part, but not all, of the time difference between the peaks. The remaining difference is probably caused by the response function and the effect of a collimator. In [9] it was shown that the peak was shifted towards shorter times if an ideal collimator was applied. Another difference between the 2D and 3D case is that the curvature of the pipe should be included.

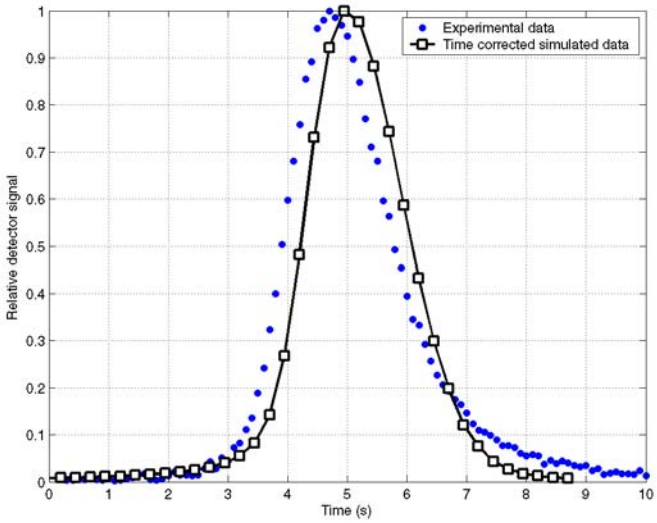

Figure 17: A comparison between the simulated and experimental data after applying the correction in Eq. 7.

8. Conclusion and discussion

A model for PNA evaluation is suggested in this work. Developments were made in the transport and mixing of the activity where a CFD code was used for the first time in a model of the PNA flowmeter. With the CFD code, the position and shape of the activity distribution at different times could be studied. The average velocity of the activity was also calculated and the results showed that there is a substantial discrepancy between the average velocity of the water and the average velocity of the activity. The discrepancy is dependent largely on the gradient in the initial activity distribution.

To evaluate PNA experiments, experimental data has to be treated properly. Background radiation is a problem in many nuclear applications and the PNA flowmeter is no exception. The background in the PNA measurement has been dealt with in different ways by different authors. The background in a PNA measurement changes both the shape and position of the peak and if not treated correctly it will decrease the accuracy of the flowmeter. A method for identifying the origin of the background as well as a method for subtracting it was developed in this work.

The prospects of developing the PNA flowmeter to a competitive flowmeter have been improved by the results in this thesis, but to make it competitive with other non-intrusive flowmeters the accuracy should be aimed at 1%. To achieve this, development of a numerical model which can explain the experimental data is needed. Most improvements should be possible in the parts involving the transport of the activity and the detection of the photons from the activity. Using CFD, which was done in this work, will then give accurate results if the initial activity distribution can be properly modelled.

9. Acknowledgement

I would like to thank my colleagues at the Department of Nuclear Engineering/Reactor Physics and other people who have directly or indirectly contributed to this work.

Special thanks goes to my supervisor Anders Nordlund for his knowledge, support and enthusiasm.

I would also like to thank Professor Imre Pázsit, our technicians Lennart Norberg and Lasse Urholm and my co-author Berit Dahl.

My previous room-mate and co-author Farshid Owrang as well as my present room-mate Elisabeth Tengborn have made the work more enjoyable.

I am grateful to Professor emeritus Nils Göran Sjöstrand for checking manuscripts, our secretary Eva Streijffert for the administrative work and Margareta and Thomas Wilhelmi for the German translation.

Thanks also to my past and present colleagues Kalle Sunde, Johanna Wright, Christophe Demazière, Chiara La Tessa, Davide Mancusi, József Bánáti, Lembit Sihver, Roumiana Chakarova, Vasily Arzhanov and Zhifeng Kuang who have all contributed to the good atmosphere at the department.

Per Lindén is acknowledged for helping me getting started with the project.

Much support has also come from family and friends: my parents, Cecilia Sönströd, Lena, Anders, Frida and Axel Assmundsgård.

Financial support from Göteborg Energi Forskningsstiftelse, The Swedish Centre for Nuclear Technology, The Swedish Centre for Nuclear Technology and The OECD Halden Project are gratefully acknowledged.

10. References

1. Boswell,C.R., Pierce, T.B.: Flowrate determination by neutron activation analysis, Proceedings of the International Conference on Modern Development in Flow Measurements,p. 264-272, Peter Peregrinus Ltd., London, UK, 1972, ISBN 0901223301
2. Drozdowicz, K.: Experiments for Water-Flow Measurements by Pulsed-Neutron Activation, CTH-RF-106, Chalmers University of Technology, Göteborg, Sweden, 1994
3. Lindén, P.; Pázsit, I.: Study of the Possibility of Determining the Mass Flow of Water from Neutron Activation Measurements with Flow Simulations and Neural Networks, Kerntechnik 63 (1998) 188
4. Grosshög, G.; Pázsit, I.; FlowAct, a Neutron Activation Method for the Measurement of Feed-Water Flow, Proc. at SMORN VII, A symposium on nuclear reactor surveillance and diagnostics, p. 492, 19-23 June, 1995, Avignon, France, Published by OECD, 1996

5. Nordlund, A.; Avdic, S.; Kaiser, N.: Study of the possibility of high accuracy flow measurements with the pulsed neutron activation method, Kerntechnik 66 (2001) 37
6. Mattsson, H., Owrang, F., Nordlund, A.: Simulation of pulsed neutron activation for determination of water flow in pipes, Kerntechnik, Vol. 67, No. 2-3 (2002) 78
7. P. Lindén and I. Pázsit, Measurement of Mass Flow of Water with Pulsed Neutron Activation and Neural Networks - the Flow Act Method, (Paper No. 196). Proc. International Conference on the Physics of Nuclear Science and Technology, Long Island, New York, U.S.A. October 1998
8. Lindén, P.; Grosshög, G.; Pázsit, I.: FlowAct, Flow Rate Measurements in Pipes with the Pulsed Neutron Activation Method, Nuclear Technology 124 (1998) 31
9. Mattsson, H., Nordlund, A.: CFD Simulation of the Pulsed Neutron Activation Technique for Water Flow Measurements, Proceedings of American Nuclear Society, France 2005
10. Mattsson, H., Nordlund, A., Evaluation of the Pulsed Neutron Activation Method using CFD, Proceedings of PSFVIP-5, Australia, 2005
11. Mattsson, H., Nordlund, A., CFD Simulation of the Pulsed Neutron Acitvation Technique for Water Flow Measurements, Proceedings of American Nuclear Society, France 2005
12. Olsson, D., Cross correlation in water flow, Diploma work, CTH-RF-172, Chalmers University of Technology, Gothenburg, Sweden, 2003
13. Lindén, P.: Water Flow Measurements with the Pulsed Neutron Activation Method, Licentiate thesis, CTH-RF-129, Chalmers University of Technology, Göteborg, Sweden, 1997
14. Avdic, S.: Development of Neutron Measurement Techniques in Reactor Diagnostics and Determination of Water Content and Water Flow, Licentiate thesis, CTH-RF-155, Chalmers University of Technology, Gothenburg, Sweden, 2000
15. Mattsson, H., Developments in Pulsed Neutron Activation for Determination of Water Flow in Pipes, Licentiate thesis, CTH-RF-171, Chalmers University of Technology, Gothenburg, Sweden, 2003
16. Lindén, P.:, A Study of Using Pulsed Neutron Activation for Accurate Measurements of Water Flow in Pipes, Doctoral Thesis, Chalmers University of Technology, Göteborg. Sweden, 1998, ISBN 91-7197-739-2
17. Uno,Y. et al.: Absolute measurement of D-T neutron flux with a monitor using activation of flowing water, Fusion Engineering and Design 56-57 (2001) 895
18. Kaneko, J et al.: Technical feasibility study on a fusion power monitor based on activation of water flow, Review of Scientific Instruments Vol. 72, No. 1 (2000) 809
19. Johnson, L.C. et al.: Analysis of neutron cameras for ITER, Review of Scientific Instruments, Vol. 70, No. 1 (1999) 1145
20. Lahey, R.T, Jr.: A review of Some Selected Nonintrusive Nuclear and Optical Techniques for the Determination of Void Fraction, Flow Regime and Two-Phase Flow, Trans. Am. Nucl. Soc. 39, (1981) 1006
21. Perez-Griffo, M.L., Block R.C., Lahey R.T. Jr., 16N Tagging for Two-Phase Mass Flow Measurements, Trans. Am. Nucl. Soc. 30 (1978) 500
22. Kehler, P.: Pulsed neutron measurement of single and two-phase liquid flow, IEEE Transactions on Nuclear Science NS-26, No. 1 (1979) 1627
23. Hsu, Y.Y., Kondic, N., Solbrig, C.: Multiple Gamma-Beam Attenuation, Tracers, Activation, and Light/Optical Techniques in Two-Phase Flow Measurement, Trans. Am. Nucl. Soc. 39 (1981) 1000

24. Larson, H.A., Price, C.C., Curran, R.C., Sackett, J.I.: Flow measurements in sodium and water using pulsed-neutron activation: Part 1, Theory, Nuclear Technology, Vol. 57, no. 2, p. 264-271, May, 1982
25. Price, C.C.; Larson, H.A.; Curran, R.N.; Sackett, J.I.: Flow measurement in sodium and water using pulsed-neutron activation: Part 2, Experiment, Nuclear Technology 57, (1982) 272
26. Browne, E.; Firestone, R.B.; Shirley, S.S.: Table of Radioactive Isotopes, John Wiley & Sons, New York, 1986, ISBN 0-471-84909-X
27. McLane, V., Dunford, C.L., Rose, P.F.: Neutron Cross Sections, Vol. 2, Academic Press, Inc., USA, 1988, ISBN 0-12-484220-8
28. T-2 Nuclear Information Services, Los Alamos National Laboratory, University of California, USA. Available at http://t2.lanl.gov/
29. Knoll, G.F., Radiation detection and measurement, Second edition, John Wiley & Sons, Singapore, 1989
30. Taylor, G.I.: Dispersion of soluble matter in turbulent flow through a tube, Proc. R. Soc. A, Vol. 223 (1953) 446
31. Perez-Griffo, M.L.; Block, R.C.; Lahey, R.T. Jr.: Measurement of Flow in Large Pipes by the Pulsed Neutron Activation Method, Nuclear Science and Engineering 82, (1982) 19
32. Taylor, G.I.: Dispersion of soluble matter in solvent flowing slowly through a tube, Proc. R. Soc. A, Vol. 223 (1953) 186
33. Coulson, J.M.; Richardson, J.F.; Backhurst, J.R.; Harker, J.H.: Chemical Engineering, Vol. 1, Fourth Edition, Pergamon Press, Oxford, 1990, ISBN 0-08-037948-6
34. Tritton, D.J.: Physical Fluid Dynamics, Second edition, Oxford University Press, Great Britain, 2001, ISBN 0-19-854493-6
35. Fluent 6.1 User's Guide, Fluent Inc., Lebanon, USA
36. Achard, J.L.; Delhaye, J.M.: Modeling aspects of the PNA technique for flow rate measurements, Thermal-Hydraulics of Nuclear Reactors. Sec. Intl. Top. Meeting on Nucl. Reac. Th.-Hydl. S:a Barbara, Calif., USA, 11-14 Jan., 1983, Vol. 2, p. 1456 ANS, USA, 1983
37. Gardner, R.P.; Barrett, C.L.; Haq, W.; Peplow, D.E.: Efficient Monte Carlo Simulation of 16O Neutron Activation and 16N Decay Gamma-Ray Detection in a Flowing Fluid for On-Line Oxygen Analysis or Flow Rate Measurement, Nuclear Science and Engineering 122 (1996) 326
38. Perez-Griffo, M.L.; Block, R.C., Lahey R.T Jr., A Mechanistic Analysis of LOFT Pulsed Neutron Activation Data, Trans. Am. Nucl. Soc. 38 (1981) 750